



## Designing stable ABR flow control with rate feedback and open-loop control: first-order control case <sup>☆</sup>

Song Chong <sup>a,\*</sup>, Ramesh Nagarajan <sup>b</sup>, Yung-Terng Wang <sup>b</sup>

<sup>a</sup> Department of Electronic Engineering, Sogang University, Seoul 121742, South Korea

<sup>b</sup> Performance Analysis Department, Bell Laboratories, Holmdel, NJ 07733, USA

---

### Abstract

In this paper we present a control-theoretic approach to design stable rate-based flow control for ATM ABR services. The flow control algorithm that we consider has the most simple form among all the queue-length-based flow control algorithms, and is referred to as *first-order rate-based flow control* (FRFC) since the corresponding closed loop can be modeled as a first-order retarded differential equation. We analyze the equilibrium and the asymptotic stability of the closed loop for the case of multiple connections with diverse round-trip delays. We also characterize the asymptotic decay rate at which the stable closed loop tends to the equilibrium. The decay rate is shown to be a concave function of control gain with its maximum being the inverse of round-trip delay. We also consider an open loop control in which the queue control threshold is dynamically adjusted according to the changes in the available bandwidth and the number of connections. This open loop control is shown to be necessary and effective to prevent the closed loop from converging to an undesirable equilibrium point. ©1998 Elsevier Science B.V. All rights reserved.

*Keywords:* ATM networks; ABR flow control; Explicit rate allocation; Asymptotic stability; Fairness

---

### 1. Introduction

Recently there has been a great interest in feedback-based flow control for high-speed wide-area ATM networking. In particular, a *rate-based approach* has been studied extensively [2–11,15–20] and adopted by the ATM Forum as the standard for the flow control of the available bit rate (ABR) service [4,12].

The rate-based flow control problem in high-speed wide-area ATM networks can be stated as follows. Consider a network with a single bottleneck link as depicted in Fig. 1. The geographically distributed sources transmit data into the bottleneck node in their path at the rate allocated by the node. In reality, the

---

<sup>☆</sup> An earlier version of this paper was presented at the Performance and Control of Network Systems Conference, Wai Sum Lai, Hisashi Kobayashi (Eds.), Proceedings of SPIE (The International Society for Optical Engineering), vol. 3231, Dallas, TX, 3–5 November 1997. This work was carried out in part while Song Chong was with the Performance Analysis Department at Bell Laboratories, Holmdel, NJ and supported in part by Korea Science and Engineering Foundation under grant 971-0905-032-2.

\* Corresponding author. Tel.: +82-2-705-8473; fax: +82-2-706-4216; e-mail: chsong@ccs.sogang.ac.kr.

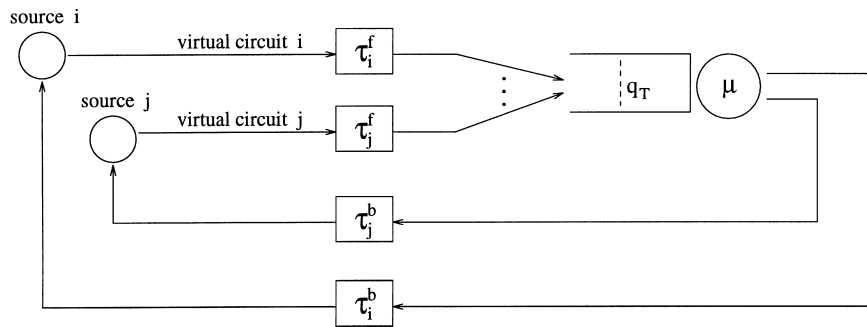


Fig. 1. Network model with a single bottleneck link.

bottleneck can be any node in the network and for simplicity, we consider only a single link in the network as a bottleneck. The switch computes the rates that will be allocated to the sources. In the queue-length-based rate control that we consider in this paper, the rates are computed based on a certain function of the difference between the observed queue length and a queue threshold. In this type of approach, a certain fairness in rate allocation among users is accomplished as a consequence of the queue-length control. Examples of this type can be found in [2,5–8,11,15–20]. The other type of rate-based flow control [3,10] is to compute directly rate allocations in a way that a certain fairness property is satisfied. Typically, in this latter approach, the queue length is not explicitly controlled. Communication between the node and the sources is done via special cells that are embedded into the individual data streams. It is well understood that the large bandwidth-delay product involved in the problem can cause a loose control with non-negligible loss and link under-utilization.

There are important criteria in the design of high-performance ABR flow control algorithms. In the following, we summarize the criteria in consideration in this paper.

- Maximal link utilization and small cell loss, and consequently maximal throughput in steady state.
- Stability (preferably asymptotic stability) of the steady-state solution for the case of multiple virtual circuits (VCs) with long and diverse round-trip delays.
- Fair bandwidth allocation among ABR streams; guarantee of standard fairness criteria such as *MAX-MIN fair share* [12].
- Fast and uniform convergence irrespective of number of active VCs.
- Adaptability to the changes in the operational environment, for instance, changes in available bandwidth and the number of active VCs.
- Simplicity in implementation.

As a solution to meet these criteria, we consider a control-theoretic rate-based flow control algorithm which we first proposed in [6] and refer to as *first-order rate-based flow control* (FRFC). The FRFC is a queue-length-based flow control algorithm where the rate allocated to each ABR user is the difference between observed network queue length and queue threshold, multiplied by a control gain. In contrast, most other existing queue-length-based algorithms [2,5,7,8,11,16–20] control the derivative of the rate as a certain function of queue length and thus is viewed as a second-order rate control. The intent of this paper is to explore the capability and develop a theoretical foundation of the first-order control as an alternative solution, and not to claim that the first-order control is more adequate than the second-order control for ABR flow control purpose.

The analysis in the paper will show that when the FRFC is applied, the ABR closed loop consisting of multiple VCs with diverse delays has two equilibrium points: one fully utilizing the available bandwidth

with the guarantee of MAX-MIN fair allocation of rates, and the other not. It will be also shown that if the control gains are properly chosen, the closed loop can be asymptotically stabilized at the desired equilibrium point for arbitrarily large delays. The asymptotic decay rate at which the stable closed loop approaches the equilibrium may be a function of the control gains. It will be shown for the special case with identical round-trip delays that the decay rate is a concave function of the average control gain and its value is at most the inverse of round-trip delay. We also consider an open loop control in which the queue control threshold is dynamically adjusted according to the changes in the available bandwidth and the number of connections. This additional control will be shown to be necessary to prevent the closed loop from converging to an undesirable equilibrium point.

The paper is organized as follows. Section 2 describes the FRFC algorithm and the closed-loop model. In Section 3, the equilibrium and the asymptotic stability of the closed loop with the FRFC are addressed. The asymptotic decay rate is analyzed in Section 4 and the open-loop control is introduced in Section 5. In Section 6 simulations are presented, and the conclusion appears in Section 7.

## 2. Closed-loop control and modeling

The assumptions employed for the analysis of the FRFC algorithm are as follows and are fairly standard [2,5–8]:

**Assumption 2.1.** The traffic is viewed as a deterministic fluid flow and the network queuing process and the feedback control is continuous in time. This assumption enables us to model the closed-loop system by a differential equation.

**Assumption 2.2.** The round-trip-time,  $\tau_i$ , of virtual circuit  $i$  is the sum of forward-path delay,  $\tau_i^f$ , and the backward-path delay,  $\tau_i^b$ , which consists of propagation, queueing, transmission and processing times. We assume that  $\tau_i$  is a constant. This is a reasonable assumption in a wide-area network where propagation delays are expected to dominate.

**Assumption 2.3.** The sources are *persistent* until the system reaches steady state. By the term persistent, we mean that the source always has enough data to transmit at the allocated rate.

**Assumption 2.4.** There are no arrivals and departures of virtual circuits until the system reaches steady state.

**Assumption 2.5.** The available bandwidth of the bottleneck link is constant until the system reaches steady state. Also, the buffer size at the bottleneck link is assumed infinite.

Assumptions 2.4 and 2.5 will be removed as necessary in Sections 5 and 6 to deal with dynamic environments.

Let  $r_i(t)$ ,  $i = 1, \dots, n$ , denote the rate allocation to virtual circuit  $i$ , which is computed by the switch at time  $t$ . Also, let  $q(t)$ ,  $\dot{q}(t)$  and  $\mu$ , respectively, denote the queue length, its derivative at time  $t$ , and the available bandwidth at the bottleneck link. The rate-based flow control algorithm that we consider in this paper is a switch algorithm of the following simple form:

$$r_i(t) = \left( -\frac{K_i}{n}(q(t) - q_T) \right)^+, \quad K_i > 0, \quad (1)$$

where  $K_i$  is the control gain,  $q_T$  is the queue length threshold for the flow control, and the symbol  $(\cdot)^+$  denotes  $\max\{\cdot, 0\}$ . We refer to this algorithm as *first-order rate-based flow control* (FRFC) since as we will see, the behavior of the closed-loop system with this form of algorithm is governed by a first-order differential equation. In contrast, most other existing algorithms found in [2,5,7,8,11,16–20] can be viewed as a second-order flow control since the rate is modulated via its derivative and thus the behavior of the closed-loop system is governed by a second-order differential equation. For instance, the algorithm in [7,8] has the following form:

$$\dot{r}_i(t) = -a_i r_i(t) - b_i (q(t) - q_T), \quad (2)$$

where  $a_i$  and  $b_i$  are two positive control constants. A noticeable feature of the FRFC algorithm is the control gain  $K_i$  scaled by the number of VCs  $n$ . It will be shown later that such a scaling can yield a uniform convergence rate of the bottleneck queue irrespective of the number of VCs. It is also noted that when the FRFC algorithm is applied, the ABR queue cannot be stabilized at the value greater than or equal to  $q_T$ . In other words, as  $q(t)$  grows and exceeds  $q_T$ , the rate allocation  $r_i(t)$  becomes zero and thus with a delay the total arrival rate gets smaller than the available bandwidth at the bottleneck link. Thus,  $q(t)$  cannot stay permanently at the value greater than or equal to  $q_T$ . As we will see,  $q(t)$  has only two equilibrium states; one at a positive value smaller than  $q_T$  and the other at zero depending on the network operational environment and the choice of the control gain parameters.

According to the above assumptions, the queuing process at the bottleneck link is given as

$$\begin{aligned} \dot{q}(t) &= \sum_{i=1}^n r_i(t - \tau_i) - \mu, \quad q(t) > 0, \\ \dot{q}(t) &= \left( \sum_{i=1}^n r_i(t - \tau_i) - \mu \right)^+, \quad q(t) = 0. \end{aligned} \quad (3)$$

In the next section we investigate the equilibrium points and the asymptotic stability of Eq. (3) when the control (1) is applied.

### 3. Equilibrium and asymptotic stability

We suppose that there exist equilibrium points for the closed-loop system and let  $q_\infty$  and  $r_{i\infty}$ , respectively, denote the steady-state solution of  $q(t)$  and  $r_i(t)$ . At equilibrium, we have  $\lim_{t \rightarrow \infty} \dot{q}(t) = 0$  and thus from (3)

$$\sum_{i=1}^n r_{i\infty} - \mu = 0 \quad \text{if } q_\infty > 0, \quad (4)$$

$$\left( \sum_{i=1}^n r_{i\infty} - \mu \right)^+ = 0 \quad \text{if } q_\infty = 0, \quad (5)$$

and from (1),

$$r_{i\infty} = \left( -\frac{K_i}{n} (q_\infty - q_T) \right)^+ \quad \forall i. \quad (6)$$

First consider the case with  $0 < q_\infty \leq q_T$ . From (4) and (6), we find that if  $q_T > n\mu / \sum_{i=1}^n K_i$ ,

$$q_\infty = q_T - \frac{n\mu}{\sum_{i=1}^n K_i}, \quad r_{i\infty} = \frac{K_i}{\sum_{i=1}^n K_i} \mu \quad \forall i.$$

Next we consider the case with  $q_\infty = 0 < q_T$ . Similarly, from (5) and (6), we obtain that if  $q_T \leq n\mu / \sum_{i=1}^n K_i$ ,

$$q_\infty = 0, \quad r_{i\infty} = \frac{K_i}{n} q_T \leq \frac{K_i}{\sum_{i=1}^n K_i} \mu \quad \forall i.$$

The following proposition states the existence of equilibrium points.

**Proposition 3.1.** *For the FRFC, there exist two steady-state solutions (equilibrium points): if  $q_T > n\mu / \sum_{i=1}^n K_i$ ,*

$$q_\infty = q_T - \frac{n\mu}{\sum_{i=1}^n K_i}, \quad r_{i\infty} = \frac{K_i}{\sum_{i=1}^n K_i} \mu \quad \forall i, \quad (7)$$

otherwise,

$$q_\infty = 0, \quad r_{i\infty} = \frac{K_i}{n} q_T \leq \frac{K_i}{\sum_{i=1}^n K_i} \mu \quad \forall i. \quad (8)$$

Note that  $q_\infty$  cannot be greater than or equal to the control threshold  $q_T$ . The network queue can be stabilized at either zero or a certain value smaller than  $q_T$ . For given  $n\mu$ , the choice of  $q_T$  and  $K_i$ ,  $i = 1, \dots, n$ , determines where for the system to converge. If  $q_T$  and  $K_i$ ,  $i = 1, \dots, n$  are chosen such that  $q_T > n\mu / \sum_{i=1}^n K_i$ , the system has the equilibrium in (7) where the bottleneck link is fully utilized and any desired sharing of the bottleneck bandwidth can be accomplished through a proper selection of control gains. For instance, by taking identical gains, one can achieve MAX-MIN fair bandwidth sharing. On the other hand, if  $q_T$  and  $K_i$ ,  $i = 1, \dots, n$ , are chosen such that  $q_T \leq n\mu / \sum_{i=1}^n K_i$ , the system has the equilibrium in (8) where the bandwidth sharing can be still fair but the available bandwidth cannot be fully utilized.

Now we investigate the asymptotic stability of the equilibrium point (7) where full link-utilization is achieved. Informally, asymptotic stability implies that all trajectories of the system, in this case the queue length and consequently the source rates as well, which start within some bound of the equilibrium point remain within another bound of the equilibrium point and further the trajectory asymptotically approaches the equilibrium point. The rigorous definition of asymptotic stability of equilibrium points can be found in [1]. In the following, we analyze only the local asymptotic stability and the global asymptotic stability is investigated via simulations only. This is similar to the approach in [2]. For understanding the local stability, we can ignore the non-linearities introduced by the buffer floor and the control, and the queueing process at the bottleneck link can be written as

$$\dot{q}(t) = \sum_{i=1}^n r_i(t - \tau_i) - \mu \quad (9)$$

and

$$r_i(t) = -\frac{K_i}{n} (q(t) - q_T), \quad (10)$$

respectively. Define

$$e(t) = q(t) - q_\infty = q(t) - q_T + \frac{n\mu}{\sum_{i=1}^n K_i}. \quad (11)$$

By combining (9)–(11), we obtain the following closed-loop equation:

$$\dot{e}(t) + \frac{1}{n} \sum_{i=1}^n K_i e(t - \tau_i) = 0, \quad (12)$$

which is a first-order retarded differential equation [1,13]. The characteristic equation of the closed-loop equation (12), denoted by  $D(s)$ , is

$$D(s) = s + \frac{1}{n} \sum_{i=1}^n K_i e^{-s\tau_i} = 0, \quad (13)$$

which is an exponential polynomial of  $s$ . For *asymptotic stability* of the closed-loop equation (12), all the roots of the characteristic equation (13) must have negative real parts [1,13].

To find the necessary and sufficient condition for  $D(s) = 0$  to have stable roots, one can appeal to Pontryagin's criterion [1,8] assuming discrete delays of rational ratios. For more general case with continuous delays or discrete delays of irrational ratios, Stépán's criterion [13] provides a way to construct the necessary and sufficient condition. However, constructing such a condition in an explicit form is extremely complicated for the system with multiple connections of diverse round-trip delays.

Instead of finding the necessary and sufficient condition, we will derive a useful sufficient condition for the asymptotic stability of the equilibrium point (7). The following theorem in [13], which we re-state below for convenience, provides the means to construct the necessary condition.

**Theorem 3.2.** Consider the characteristic function  $D(s)$  given by

$$D(s) = \sum_{i=0}^d (-1)^i a_i(s) s^{d-i}. \quad (14)$$

Suppose that there exist the polynomials  $R^+$ ,  $R^-$ ,  $S^+$  and  $S^-$  such that

$$R^-(\omega) \leq R(\omega) = \operatorname{Re} D(i\omega) \leq R^+(\omega), \quad (15)$$

$$S^-(\omega) \leq S(\omega) = \operatorname{Im} D(i\omega) \leq S^+(\omega), \quad (16)$$

for  $\omega \in [0, \infty)$ . Suppose that  $R^+$  and  $R^-$  have the same number of real positive zeros. These zeros are denoted by  $\rho_1^+ \geq \dots \geq \rho_p^+ > 0$  and  $\rho_1^- \geq \dots \geq \rho_p^- > 0$  and they determine the intervals  $I_{Rl} = [\min\{\rho_l^-, \rho_l^+\}, \max\{\rho_l^-, \rho_l^+\}]$  ( $l = 1, \dots, p$ ). In exactly the same way, the zeros of  $S^+$  and  $S^-$  define the intervals  $I_{Sj}$  ( $j = 1, \dots, q$ ). Furthermore, let all these intervals be disjoint and let us choose the representative real numbers  $\rho_l^0 \in I_{Rl}$  ( $l = 1, \dots, p$ ) and  $\sigma_j^0 \in I_{Sj}$  ( $j = 1, \dots, q - 1$ ).

All the roots of the characteristic equation  $D(s) = 0$  have negative real parts if

$$d = 2m,$$

$$S(\rho_l^0) \neq 0, \quad l = 1, \dots, p,$$

$$\sum_{l=1}^p (-1)^l \operatorname{sgn} S(\rho_l^0) = (-1)^m m \quad (17)$$

or

$$d = 2m + 1,$$

$$R(\sigma_j^0) \neq 0, \quad j = 1, \dots, q - 1,$$

$$R(0) > 0,$$

$$\sum_{j=1}^{q-1} (-1)^j \operatorname{sgn} R(\sigma_j^0) + \frac{1}{2}((-1)^q + (-1)^m) + (-1)^m m = 0, \quad (18)$$

where  $m$  is integer and the symbol  $\operatorname{sgn}$  denotes sign function.

The above theorem yields the following result.

**Proposition 3.3.** *The closed-loop system (12) is asymptotically stable if  $(1/n) \sum_{i=1}^n K_i \tau_i < 1$ .*

**Proof.** From (13), we have  $d = 1$  ( $m = 0$ ) and

$$R(\omega) = \frac{1}{n} \sum_{i=1}^n K_i \cos(\omega \tau_i), \quad S(\omega) = \omega - \frac{1}{n} \sum_{i=1}^n K_i \sin(\omega \tau_i). \quad (19)$$

Since  $K_i > 0 \forall i$ , the second condition in (18),  $R(0) > 0$ , is satisfied. On the other hand, one can estimate  $S(\omega)$  in the following way:

$$S(\omega) > S^-(\omega) = \left(1 - \frac{1}{n} \sum_{i=1}^n K_i \tau_i\right) \omega, \quad \omega \in (0, \infty), \quad (20)$$

since  $\sin(\omega \tau_i) < \omega \tau_i$  for  $\omega \in (0, \infty)$ . If  $(1/n) \sum_{i=1}^n K_i \tau_i < 1$ , it is obvious that  $S(\omega)$  has no real positive zeros since it is positive for  $\omega \in (0, \infty)$ . Thus, no  $\sigma_j^0$ s exist and hence the first and the second stability conditions in (18) are degenerated, independently from the polynomial estimation of  $R(\omega)$ . Theorem 3.2 implies the statement of the proposition.  $\square$

Since the above condition for stability is only a sufficient condition, the question naturally arises as to its tightness. Consider the case that  $K_i = K \forall i$ . In this case, the condition implies that  $K < \bar{\tau}^{-1}$  where  $\bar{\tau}$  is the average round-trip delay of all the active VCs, i.e.,  $\bar{\tau} = (1/n) \sum_{i=1}^n \tau_i$ . It will be shown in the next section that the closed-loop system converges nearly exponentially with the decay rate closely related to the value of the gain  $K$ . Since any reactive feedback-based flow control scheme in a wide-area network can only be expected to converge to the equilibrium point as fast as the average round-trip delay will permit, we hence conjecture that the condition for asymptotic stability is fairly tight in spite of being only a sufficient condition. The simulation studies in Section 6 will provide further evidence of the fast convergence even when the control parameters are set in accordance with the potentially restrictive sufficient condition. In addition, it is very difficult to find a sufficient and necessary condition, in an explicit form that is readily applicable, for the case of multiple connections with diverse round-trip delays [13]. In contrast,

the condition in Proposition 3.3 is easy to use and requires only the estimate of average round-trip delay if identical gains are chosen.

Next we derive the necessary and sufficient condition for asymptotic stability for a special case that all the round-trip delays are identical. Let  $\tau_i = \tau \forall i$ . Then, the closed-loop equation (12) becomes

$$\dot{e}(t) + \frac{1}{n} \sum_{i=1}^n K_i e(t - \tau) = 0. \quad (21)$$

This equation may be normalized so that the time lag  $\tau$  is unity. Let  $t = \tau\xi$ . In terms of the new variable  $\xi$ , (21) becomes

$$\dot{e}(\xi) + Pe(\xi - 1) = 0, \quad (22)$$

where

$$P = \frac{\tau}{n} \sum_{i=1}^n K_i. \quad (23)$$

The characteristic equation of (22), denoted by  $H(z)$ , is

$$H(z) = ze^z + P = 0. \quad (24)$$

For asymptotic stability of the closed-loop equation (22), all the roots of (24) must have negative real parts. To find the necessary and sufficient condition for  $H(z) = 0$  to have such roots, one can appeal to Pontryagin's criterion [1,8], which we re-state below for convenience.

**Theorem 3.4.** *Consider the exponential polynomial*

$$H(z) = \sum_{l=0}^L \sum_{m=0}^M b_{lm} z^l (e^z)^m = 0 \quad (25)$$

with the principal term  $b_{LM} z^L (e^z)^M$ . Let  $F(\omega) = \text{Re } H(i\omega)$ ,  $G(\omega) = \text{Im } H(i\omega)$ . In order for all the zeros of  $H(z)$  to have negative real parts, it is sufficient and necessary that:

- (i)  $G(\omega)$  [or  $F(\omega)$ ] has exactly  $4kL + M$  real zeros in the interval  $-2k\pi + \epsilon \leq \omega \leq 2k\pi + \epsilon$  starting with sufficiently large  $k$ ,  $\epsilon$  being some appropriate constant.
- (ii) For each zero of  $G(\omega)$  [or  $F(\omega)$ ], to be denoted by  $\omega_i$ ,

$$F(\omega_i) \dot{G}(\omega_i) > 0, \quad [\text{or, } -\dot{F}(\omega_i) G(\omega_i) > 0]. \quad (26)$$

The above theorem yields the following result.

**Proposition 3.5.** *The closed-loop system (21) is asymptotically stable if and only if  $(\tau/n) \sum_{i=1}^n K_i < \pi/2$ .*

**Proof.** From (24), we have  $L = 1$ ,  $M = 1$  and

$$F(\omega) = -\omega \sin \omega + P, \quad (27)$$

$$G(\omega) = \omega \cos \omega. \quad (28)$$

First we show that  $G(\omega)$  satisfies the condition (i). If we take  $k = 1$  and  $\epsilon = 0$ , then  $G(\omega)$  has five real zeros in the interval  $[-2\pi, 2\pi]$  including  $\omega = 0$  as required. If we increase  $k$  from 1 to 2, the total number of real zeros in the interval  $[-4\pi, 4\pi]$  increases by 4 and hence becomes 9. In the same manner, the total number of real zeros of  $G(\omega)$  in the corresponding interval continues to increase by 4 as  $k$  increases by 1. Therefore,  $G(\omega)$  has the appropriate number of real zeros as required. Next we find the condition on  $P$  to satisfy the condition (ii). Since  $\dot{G}(\omega) = \cos \omega - \omega \sin \omega$ , the following inequality must apply to all zeros of  $G(\omega)$ :

$$(-\omega \sin \omega + P)(\cos \omega - \omega \sin \omega) > 0. \quad (29)$$

For  $\omega = 0$ , (29) implies that  $P > 0$ , which is obvious from our assumption that  $K_i > 0 \forall i$ . For non-zero zeros of  $G(\omega)$ , it must be satisfied that

$$\cos \omega = 0. \quad (30)$$

Therefore, non-zero zeros of  $G(\omega)$ , say  $\{\omega_i\}$ , can be written by

$$\omega_i = \frac{\pi}{2} + i\pi, \quad i = 0, \pm 1, \pm 2, \dots \quad (31)$$

By applying (30) and dividing both sides by  $\omega^2 \sin^2 \omega$ , the inequality (29) implies that

$$\frac{P}{\omega \sin \omega} < 1. \quad (32)$$

Note that the inequality (32) is satisfied for all non-zero zeros  $\{\omega_i\}$  of  $G(\omega)$  given in (31) if and only if it is satisfied for  $\omega_0 = \pi/2$  (or  $\omega_1 = -\pi/2$ ). Hence, we conclude that the Pontryagin's condition (ii) is satisfied if  $P = (\tau/n) \sum_{i=1}^n K_i < \pi/2$ .  $\square$

The stability condition given in Proposition 3.5 is the sufficient and necessary condition for the special case with homogeneous delays, whereas the condition given in Proposition 3.3 is only a sufficient condition for the general case with heterogeneous delays. Consider the case that  $\tau_i = \tau$ ,  $K_i = K \forall i$ . In this case, these two conditions imply that  $K < \tau^{-1}$  and  $K < (\pi/2)\tau^{-1}$ , respectively, i.e., the actual range of stable  $K$  is larger than the range given by the sufficient condition by the factor  $\pi/2$ . Therefore we can argue that the stability condition in Proposition 3.3 is fairly tight in spite of being only a sufficient condition.

The above stability analysis technique can also be applied to higher-order flow control problems. In [7] we have derived a sufficient condition for the asymptotic stability of a class of second-order flow control algorithms such as the one in (2) for the case of multiple VCs with diverse delays. Also, in [8] the Pontryagin's criterion [1] has been applied to the second-order flow control problem.

#### 4. Asymptotic decay rate and dependence on control gain

In this section we determine the rate at which the stable closed-loop system approaches steady state. Consider the principal root  $z^*$ , which is the root of (24) having the largest real part. Let  $\alpha = -\text{Re}(z^*) > 0$ . Then, the asymptotic solution of the closed-loop equation (22) satisfies the following inequality:

$$\lim_{\xi \rightarrow \infty} |e(\xi)| \leq C e^{-\alpha \xi}, \quad (33)$$

where  $C$  is a properly chosen positive real constant taking into account initial conditions. In terms of the original variable  $t (= \tau\xi)$ , (33) can be rewritten by

$$\lim_{t \rightarrow \infty} |e(t)| \leq Ce^{-(\alpha/\tau)t}. \quad (34)$$

Note that  $\alpha/\tau$  is the asymptotic decay rate at which the system tends to the equilibrium point. Hence the inverse of it,  $\tau/\alpha$ , is the time constant of the closed-loop system, i.e., the time it takes for a small perturbation around the equilibrium point to decrease by a factor of  $e^{-1}$ . Consider the case that  $\tau_i = \tau \forall i$ . The change of variable  $z = \psi - \sigma\tau$  transforms the characteristic equation (24) to

$$(\psi - \sigma\tau)e^\psi + Pe^{\sigma\tau} = 0. \quad (35)$$

If we choose  $\sigma$  to be the supremum of positive real number for which the transformed characteristic equation (35) has all roots in the left half plane, then  $\alpha = \sigma\tau$ , and the asymptotic decay rate and the time constant are  $\sigma$  and  $\sigma^{-1}$ , respectively. The sufficient and necessary conditions that all roots of a characteristic equation in the form of (35) be in the left half plane were given by earlier works in [14]. We re-state these conditions as a set of inequalities:

$$\sigma\tau < 1, \quad (36)$$

$$\sigma\tau e^{-\sigma\tau} < P, \quad (37)$$

$$P < \frac{u_1}{\sin u_1} e^{-\sigma\tau}, \quad (38)$$

where  $u_1$  is the root of the equation

$$u = \sigma\tau \tan u \quad (39)$$

in the interval  $(0, \pi)$ . We now choose  $\sigma$  to be the supremum of positive real numbers satisfying (36)–(38). Inequality (38) is equivalent to

$$P < \frac{u_1}{\sin u_1} e^{-u_1/\tan u_1}. \quad (40)$$

The right-hand side of (40) is monotone increasing on  $0 < u_1 < \pi$ . It follows from (39) that  $u_1$  decreases when  $\sigma$  increases. Thus an increase in  $\sigma$  produces a decrease in the right-hand side of (40), and the maximum  $\sigma$  satisfying this inequality is obtained by solving the corresponding equality. By an analogous argument, since an increase in  $\sigma$  on  $\sigma\tau < 1$  produces an increase in the left-hand side of (37), the maximum satisfying this inequality is also obtained by solving the corresponding equality. If any of the three equalities corresponding to (36), (37) and (40) has no solution for  $\sigma$ , the corresponding inequality places no restriction on  $\sigma$ . We summarize our results as follows:

**Proposition 4.1.** Consider the stable closed-loop system (21). Let  $\sigma_1, \sigma_2, \sigma_3$  be the positive solutions of

$$\sigma\tau = 1, \quad (41)$$

$$\sigma\tau e^{-\sigma\tau} = \frac{\tau}{n} \sum_{i=1}^n K_i, \quad \sigma\tau \leq 1, \quad (42)$$

$$\frac{\tau}{n} \sum_{i=1}^n K_i = \frac{u_1}{\sin u_1} e^{-u_1/\tan u_1}, \quad u_1 = \sigma\tau \tan u_1, \quad u_1 \in (0, \pi), \quad (43)$$

respectively, with the understanding that  $\sigma_i = \infty$  if the corresponding equation has no solution. Then, the asymptotic decay rate  $\sigma$  of the closed-loop solution is given by

$$\sigma = \min\{\sigma_1, \sigma_2, \sigma_3\} \quad (44)$$

and  $\sigma \leq \tau^{-1}$ .

Note that the asymptotic decay rate is a function of only two system parameters, round-trip delay  $\tau$  and the average of control gains,  $\bar{K} = (1/n)\sum_{i=1}^n K_i$ . The decay rate is independent of the number of active VCs, which is a highly desirable property in practice since it guarantees an identical rate of convergence no matter how many VCs are active. In contrast, it can be shown that if the gain is not scaled by the number of VCs as in the control (1), the asymptotic decay rate becomes no longer independent of the number of VCs. What matters in this type of control is that one needs to estimate the maximum number of possible VCs, say  $n_{\max}$ , and the gains should be selected for this extreme case such that  $\bar{K} < \pi/(2n_{\max}\bar{\tau})$ . As a consequence, in nominal cases with  $n$  much smaller than  $n_{\max}$ , the system would converge unnecessarily slowly due to the small value of the chosen gains. Note also that the asymptotic time constant  $\sigma^{-1}$  cannot be smaller than the round-trip delay, which means that the time it takes for a small perturbation around the equilibrium point to decrease by a factor of  $e^{-1}$  is at least  $\tau$ .

Next we investigate the dependence of  $\sigma$  on  $\bar{K}$  for a given  $\tau$ . The function in the left-hand side of (42),  $\sigma\tau e^{-\sigma\tau}$ , is monotone increasing on  $0 < \sigma\tau < 1$  with minimum value 0 at  $\sigma\tau = 0$  and maximum value  $e^{-1}$  at  $\sigma\tau = 1$ . The function in the right-hand side of the first equation in (43)

$$g(u) \equiv \frac{u}{\sin u} e^{-u/\tan u} \quad (45)$$

is monotone increasing on  $0 < u < \tau$  with  $g(0) = e^{-1}$ ,  $\lim_{u \rightarrow \pi} g(u) = \infty$ . Also, the function in the second equation in (43),  $u/\tan u$ , is monotone decreasing on  $0 < u < \pi$  with  $\lim_{u \rightarrow 0} = 1$ . For a given  $\tau$ , define

$$K^* = e^{-1}\tau^{-1}, \quad K^{**} = g\left(\frac{\pi}{2}\right)\tau^{-1} = \frac{\pi}{2}\tau^{-1}. \quad (46)$$

Consider the case  $0 < \bar{K} < K^*$ . Since  $\bar{K} < K^*$  implies that  $(\tau/n)\sum_{i=1}^n K_i < e^{-1}$  and  $g(u_1) > e^{-1}$  for  $u_1 \in (0, \pi)$ , (43) has no solution, i.e.,  $\sigma_3 = \infty$ . On the other hand, since the function  $\sigma\tau e^{-\sigma\tau}$  is monotone increasing on  $0 < \sigma\tau < 1$  with minimum value 0 at  $\sigma\tau = 0$  and maximum value  $e^{-1}$  at  $\sigma\tau = 1$ , (42) has a unique solution  $\sigma_2$  which is smaller than  $\tau^{-1}$ . Hence,  $\sigma = \sigma_2 < \tau^{-1}$  in this case. Differentiation of (42) with respect to  $\bar{K}$  gives

$$\frac{d\sigma}{d\bar{K}} = \frac{1}{e^{-\sigma\tau}(1 - \sigma\tau)} > 0 \quad \text{when } \sigma\tau < 1. \quad (47)$$

Therefore, we conclude that  $\sigma$  is monotone increasing with respect to  $\bar{K}$ .

Consider the case  $K^* < \bar{K} < K^{**}$ . Since this case implies that  $e^{-1} < (\tau/n)\sum_{i=1}^n K_i < \pi/2$  and the value of the function  $\sigma\tau e^{-\sigma\tau}$  is smaller than  $e^{-1}$  for  $\sigma\tau < 1$ , (42) has no solution, i.e.,  $\sigma_2 = \infty$ . Since  $g(u_1)$  is monotone increasing and the image of  $g(u_1)$  is in  $(1/e, \pi/2)$  for  $u_1 \in (0, \pi/2)$ , a unique solution  $u_1$  of the first equation in (43) exists in the interval  $(0, \pi/2)$  and is monotone increasing as  $\bar{K}$  increases. Furthermore, since the function  $u_1/\tan u_1$  is monotone decreasing with respect to  $u_1$  and the image of it,  $\sigma\tau$ , is in  $(0, 1)$  for  $u_1 \in (0, \pi/2)$ , a unique solution  $\sigma$  of the second equation in (43) exists in the interval  $(0, \tau^{-1})$  and is monotone decreasing as  $\bar{K}$  increases. It is obvious that  $\sigma = \sigma_3$  in this case.

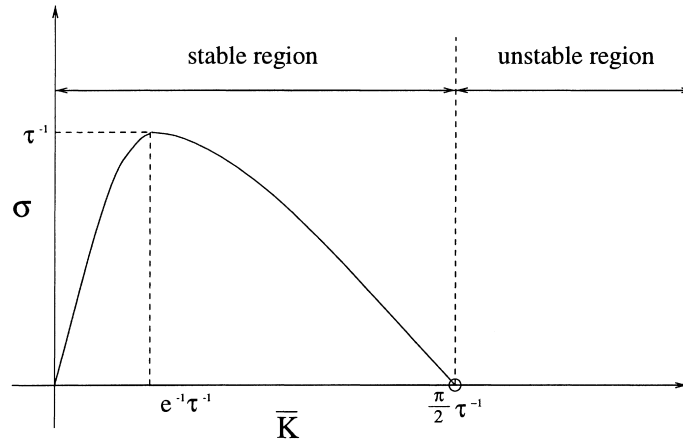


Fig. 2. Dependence of asymptotic decay rate  $\sigma$  on control gain  $\bar{K}$  for given round-trip delay  $\tau$ .

If  $\bar{K} \geq K^{**}$ ,  $(\tau/n)\sum_{i=1}^n K_i \geq \pi/2$  which implies that the closed-loop system is unstable (see Proposition 3.5). Finally, if  $\bar{K} = K^*$ ,  $(\tau/n)\sum_{i=1}^n K_i = e^{-1}$  and consequently  $\sigma = \sigma_1 = \sigma_2 = \sigma_3 = \tau^{-1}$ . We summarize our results as follows:

**Proposition 4.2.** *Consider the stable closed-loop system (21). The asymptotic decay rate  $\sigma$  is a monotone increasing function of  $\bar{K}$  given by (42) with its value being smaller than  $\tau^{-1}$  for  $0 < \bar{K} < K^*$ , and a monotone decreasing function of  $\bar{K}$  given by (43) with its value being smaller than  $\tau^{-1}$  for  $K^* < \bar{K} < K^{**}$ . Moreover,  $\sigma$  has its maximum  $\tau^{-1}$  at  $\bar{K} = K^*$ .*

Fig. 2 depicts the results of Proposition 4.2. Interestingly, the asymptotic decay rate is a concave function with respect to the average control gain, i.e., an increase in  $\bar{K}$  up to  $e^{-1}\tau^{-1}$  produces a monotone increase in  $\sigma$  but once  $\bar{K}$  exceeds a certain value,  $e^{-1}\tau^{-1}$ , the increase in  $\bar{K}$  rather produces a monotone decrease in  $\sigma$ . This is very different from the characteristics of an ordinary first-order system with no delay where the decay rate can be increased infinitely.

The above analysis considered the case with homogeneous delays. Some more analytical work is needed to understand the quantitative asymptotic behavior in the case with heterogeneous delays.

## 5. Open-loop control: getting to desired equilibrium

So far we have studied the equilibrium and the asymptotic stability of the ABR closed loop in a static environment where the bottleneck bandwidth  $\mu$  and the set of active VCs are assumed to be unchanged. In reality, however, these assumptions are no longer true. The available bandwidth at the bottleneck link is time-varying since it depends on the instantaneous aggregate traffic of higher-priority services such as CBR and VBR. Also, the set of active VCs keeps changing due to the frequent arrivals and departures of VCs. One of the major problem in such a dynamic environment is that the quantity  $n\mu/\sum_{i=1}^n K_i$  changes and hence, as shown in Proposition 3.1, the equilibrium point (i.e., the steady-state solution) of the system varies. More specifically, if  $n\mu/\sum_{i=1}^n K_i$  grows and exceeds  $q_T$  due to the changes in  $\mu$  and the set of active VCs, the link would become under-utilized and the queue would converge to zero. On the other

hand, if we choose  $q_T$  large enough to avoid such an under-utilization of link bandwidth,  $q_\infty$  would grow and so the likelihood of cell loss would increase for given buffer budget.

What is desirable in such a dynamic environment is the capability to keep  $q_T - n\mu/\sum_{i=1}^n K_i$ , i.e.,  $q_\infty$ , constant and positive. To accomplish this, we need an open-loop control in which the switch adaptively changes either  $q_T$  or the control gains whenever the changes in  $\mu$  and the set of active VCs are detected. Considering the large number of VCs in a high speed link, we choose the former option. The dynamic queue threshold (DQT) algorithm that we propose in this paper is to change the queue control threshold in the following manner:

$$q_T(t) = \frac{|I(t)| \mu(t)}{\sum_{i \in I(t)} K_i} + \epsilon, \quad \epsilon > 0, \quad (48)$$

where  $\mu(t)$  and  $I(t)$ , respectively, denote time-varying bottleneck bandwidth and the set of active VCs with cardinality  $|I(t)|$ , and  $\epsilon$  is the desired value of the ABR queue length in the steady state. For the case with  $K_i = K \forall i$ , the above DQT algorithm is simplified to

$$q_T(t) = \frac{\mu(t)}{K} + \epsilon, \quad \epsilon > 0. \quad (49)$$

Consider the closed-loop system behavior with no buffer floor when the FRFC with DQT is applied. For simplicity we assume that only  $\mu$  is time-varying while the number of VCs is fixed at  $n$ . Then, by combining (1), (3) and (48), we get the following closed-loop equation for the case with DQT

$$\dot{q}(t) + \frac{1}{n} \sum_{i=1}^n K_i q(t - \tau_i) = \frac{\epsilon}{n} \sum_{i=1}^n k_i - \mu(t) + \sum_{i=1}^n \frac{K_i}{\sum_{j=1}^n K_j} \mu(t - \tau_i). \quad (50)$$

In contrast, the closed-loop equation (12) for the case with static  $q_T$  can be rewritten as

$$\dot{q}(t) + \frac{1}{n} \sum_{i=1}^n K_i q(t - \tau_i) = \frac{q_T}{n} \sum_{i=1}^n K_i - \mu(t), \quad (51)$$

with time-varying  $\mu(t)$ . As we see in (50) and (51), the major difference between the DQT case and the static queue threshold case is the third term in the right-hand side of the DQT case (50). The role of this term is to nullify the effect of time-varying  $\mu(t)$  with delays. In particular, if  $\mu(t)$  varies slowly or is piecewise constant with reasonably long intervals, the term  $-\mu(t) + \sum_{i=1}^n (K_i / \sum_{j=1}^n K_j) \mu(t - \tau_i)$  remains small in magnitude or as a superposition of impulses so that the effect of  $\mu(t)$  becomes nearly nullified as the system approaches steady state. In contrast, with a static queue threshold, the effect of  $\mu(t)$  remains governing the dynamics of  $q(t)$  as you see in (51). This difference will result in superior performances of the FRFC with DQT in dynamic environments, as will be shown in the next section through simulations.

The connection between the closed loop control study and open loop control study is as follows: In practice the dynamics of closed loop control are expected to be faster than the dynamics of aggregate VBR traffic and the dynamics of number of active ABR VCs since individual VBR dynamics are statistically averaged and ABR VC activations are statistically counterbalanced by ABR VC deactivations due to the large number of VBR VCs and ABR VCs. Therefore, the open loop control can be viewed as an adaptive mechanism running on a timescale slower (preferably much slower) than that of the closed loop control and hence the closed loop control can be designed based on Propositions 3.3 and 3.5 as if it runs in a static environment. On the other hand, occasional occurrences of an abrupt change in the aggregate VBR traffic and/or the number of active ABR VCs can be viewed as the start point of a new control phase.

## 6. Simulation results

In this section, we simulate the network model to examine the performance of the FRFC algorithm. First we consider a static scenario where Assumptions 2.4 and 2.5 hold. The bottleneck bandwidth  $\mu$  and the buffer size  $B$  are, respectively, set to 150 Mbps and 5000 cells, and there are 50 active VCs sourcing the traffic into the link. The round-trip delay  $\tau_i$  of VCs is chosen uniformly in the range [10,40] (ms) to represent long propagation delays. To take into account the discrete-time effect of control, the FRFC is applied in the sample-and-hold manner with intervals defined by the rate of VC. We choose this interval aggressively long as if RM (resource management) cells [12] are issued every 128 data cells by the ABR sources. Fig. 3(a) shows the two steady-state solutions, (7) and (8), with  $K_i = 10.0 \forall i$ , and  $q_0 = 500$  cells. If we choose  $q_T$  at 35477 cells, the queue  $q(t)$  approaches 100 cells and the user rate  $r_i(t)$  converges to the fair allocation (= 3 Mbps) as time goes. For the illustration, the rate trajectory of a VC with 40 ms round-trip delay is plotted in the figure. On the other hand, if we choose  $q_T$  at 35277 cells,  $q(t)$  converges to 0 and  $r_i(t)$  approaches 2.9915 Mbps as computed in (8). Notice that it is not necessary for  $q_T$  to be smaller than the buffer size  $B$ .

Fig. 3(b) shows the effect of control gains on the queue and user rates with  $K_i = 10.0, 15.0$  and  $30.0$ . In the above simulation scenario, the choice of  $K_i = 10.0, 15.0$  and  $30.0$  satisfies the stability condition in Proposition 3.3 since  $1/\bar{\tau} \approx 40$ . While changing the gain, we kept  $\epsilon (= q_T - n\mu/\sum_{i=1}^n K_i)$  positive and constant at 100 cells by changing  $q_T$  correspondingly. For the larger  $K_i$ , the system suffers from poor transient behavior such as overshoots at the risk of link under-utilization and cell loss, but still remains asymptotically stable. This example tells that the sufficient stability condition that we derive can serve as a practically good gain selection criterion. In the remaining studies, we keep  $K_i = 10.0$  unless otherwise specified.

Next we consider dynamic environments where  $\mu$  and the set of active VCs are varying. For the FRFC with static threshold, we set  $q_T$  at 35877 cells aiming at  $q_\infty = 500$  cells with  $\mu(0) = 150$  Mbps. This design implies that if  $\mu$  does not vary,  $q(t)$  will converge to 500 cells. For the FRFC with DQT in (48),  $\epsilon$  was fixed at 500 cells. First, we change  $\mu(t)$  continuously in time with the derivatives of  $\pm 10$  and  $\pm 20$

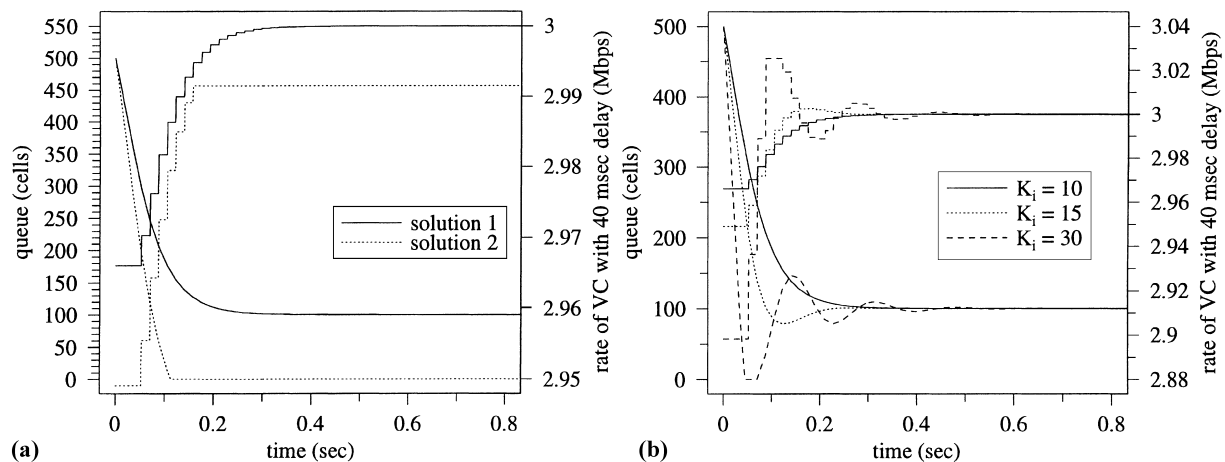


Fig. 3. Control performance in static environment ( $\mu=150$  Mbps, no. of VCs=50,  $\tau_i \in [10, 40]$  ms,  $B = 5000$  cells): (a) two steady-state solutions with  $K_i = 10.0 \forall i$ ; (b) effect of control gains  $K_i$ .

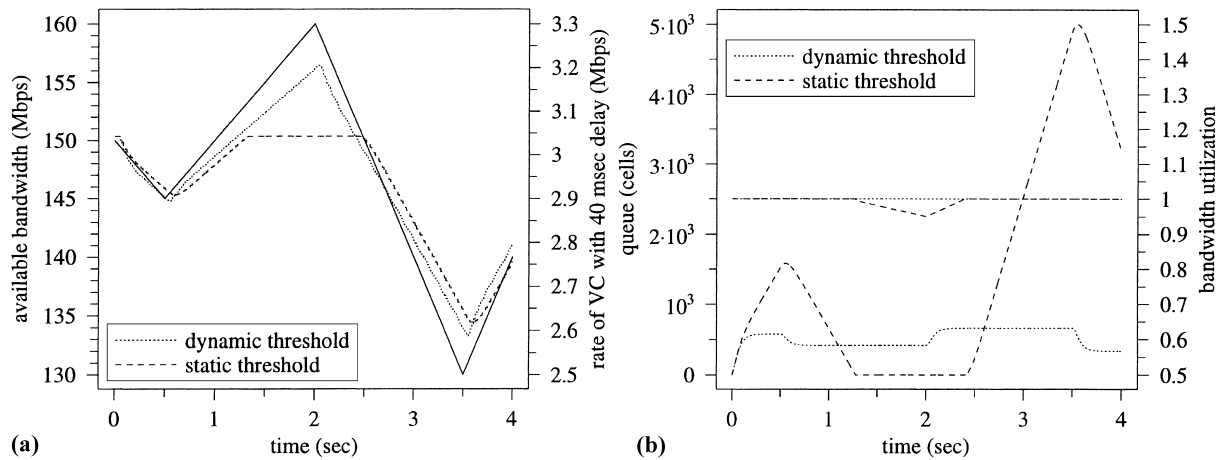


Fig. 4. Control performance when  $\mu(t)$  is continuously varying (no. of VCs = 50,  $\tau_i \in [10, 40]$  ms,  $B = 5000$  cells,  $K_i = 10.0 \forall i$ ): (a) trajectories of  $\mu(t)$  (solid curve) and  $r_i(t)$  of a VC with 40 ms round-trip delay; (b) trajectories of  $q(t)$  and bandwidth utilization.

Mbps/s and apply the FRFC with/without DQT. The trajectory of  $\mu(t)$  is plotted in Fig. 4(a) as a solid curve. Also, in Fig. 4(a), the user rate  $r_i(t)$  of a VC with longest round-trip delay ( $= 40$  ms) is compared for the two cases. With DQT  $r_i(t)$  tracks well  $\mu(t)$  with a time lag, whereas without DQT  $r_i(t)$  suffers from loss of bandwidth as observed during the time interval  $[1.25, 2.5]$  (s). Fig. 4(b) explains why such a loss of bandwidth occurs without DQT. As explained in (51), with static threshold  $q(t)$  essentially tracks the dynamics of  $-\mu(t)$ , consequently hitting both buffer floor and ceiling (see Fig. 4(b)). As also shown in Fig. 4(b), the bandwidth utilization drops while  $q(t)$  hits buffer floor, and hence the user suffers from the loss of bandwidth. On the other hand, if DQT is applied,  $q(t)$  remains in the neighborhood of  $\epsilon$  ( $= 500$  cells), maintaining full utilization of bandwidth and no loss. This is because the time-varying dynamics of  $\mu(t)$  does not directly affect the dynamics of  $q(t)$ . Rather, the difference between  $\mu(t)$  and  $\mu(t - \tau_i) \forall i$  behaves as explained in (50).

Similarly, we compare the performance of FRFC with/without DQT when  $\mu(t)$  is piecewise constant with 1 s intervals. The trajectory of  $\mu(t)$  is plotted in Fig. 5(a) as a solid curve. Exactly same observations can be made as in the previous scenario. With DQT,  $q(t)$  remains in the neighborhood of  $\epsilon$ , which is the design parameter, maintaining full utilization of bandwidth and no loss (see Figs. 5(a) and (b)). As explained in (50), it is observed in the trajectory of  $q(t)$  in Fig. 5(b) that the jumps in  $\mu(t)$  affect  $q(t)$  as impulses so that the effect of jumps vanish after a certain transient period.

Finally, we consider a dynamic scenario where VCs arrive and depart. For simplicity we keep  $\mu$  constant at 150 Mbps. For the FRFC with static threshold, we set  $q_T$  at 35877 cells aiming at  $q_\infty = 500$  cells with the given  $I(0)$ . This design implies that if  $I(t)$  does not change,  $q(t)$  will converge to 500 cells. For the FRFC with DQT in (48),  $\epsilon$  was fixed at 500 cells. The trajectory of arrival/departure of VCs is plotted in Fig. 6(a) as a solid curve. Initially there are 50 VCs, 5 VCs simultaneously arrive at 1, 2 and 3 VCs depart at 3 s. Also, in Fig. 6(a),  $r_i(t)$  of three representative VCs, respectively, arriving at 0, 1 and 2 s are shown only for the case with DQT. It is observed that the rates quickly converge to the fair share of the available bandwidth upon arrival and departure of VCs. The trajectories of  $q(t)$  and the bandwidth utilization are found in Fig. 6(b). Again, the FRFC with DQT outperforms the FRFC without DQT maintaining no loss, full utilization of available bandwidth and small queue. The spikes in  $q(t)$  found in the case of the

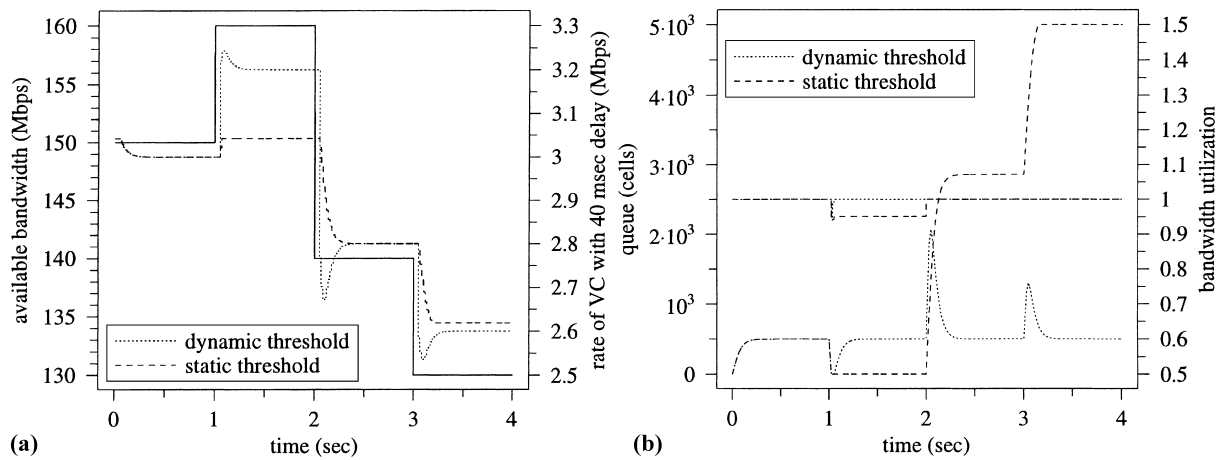


Fig. 5. Control performance when  $\mu(t)$  is piecewise constant (no. of VCs = 50,  $\tau_i \in [10, 40]$  ms,  $B = 5000$  cells,  $K_i = 10.0 \forall i$ ): (a) trajectories of  $\mu(t)$  (solid curve) and  $r_i(t)$  of a VC with 40 ms round-trip delay; (b) trajectories of  $q(t)$  and bandwidth utilization.

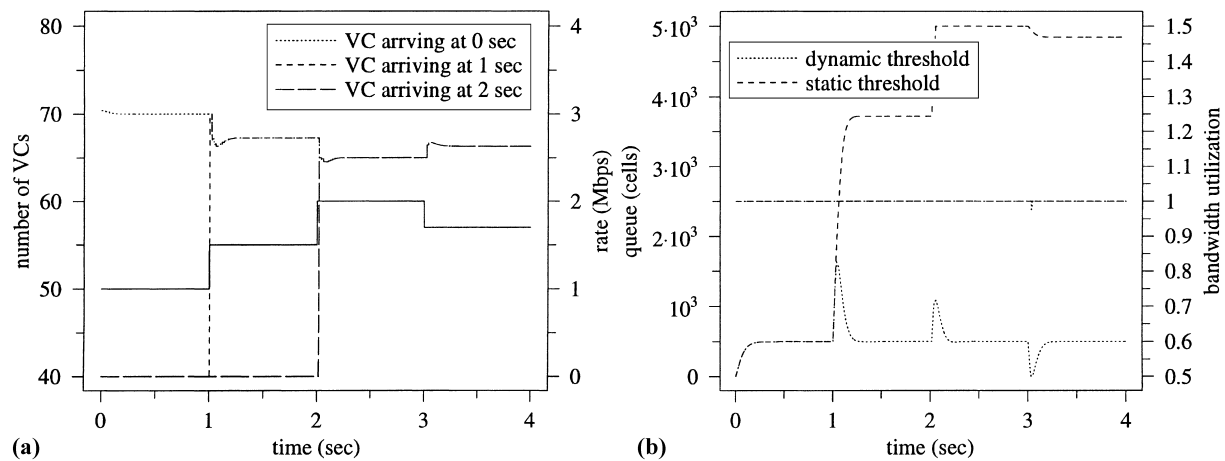


Fig. 6. Control performance upon arrivals and departures of VCs ( $\mu = 150$  Mbps,  $\tau_i \in [10, 40]$  ms,  $B = 5000$  cells,  $K_i = 10.0 \forall i$ ): (a) trajectories of number of VCs (solid curve) and  $r_i(t)$  of VCs arriving at 0, 1, 2 s in the case of FRFC with DQT; (b) trajectories of  $q(t)$  and bandwidth utilization.

FRFC with DQT is due to the simultaneous arrivals of VCs. In practice, these spikes can be mitigated by applying a ceiling to  $r_i(t)$ s at the source point to restrict the rates, but at the cost of longer transient period.

## 7. Conclusion

In this paper we have presented a control-theoretic approach to design stable rate-based flow control for ATM ABR services. The flow control algorithm that we have considered has the most simple form among all the queue-length-based flow control algorithms. We have analyzed the equilibrium and the asymptotic stability of the ABR closed loop for the case of multiple connections with diverse round-trip

delays. Two useful stability conditions have been derived: one is a sufficient condition for the general case with heterogeneous delays and the other is the necessary and sufficient condition for the special case with homogeneous delays. We have also characterized the asymptotic decay rate at which the stable closed loop tends to the equilibrium. The decay rate has been shown to be a concave function of control gain with its maximum being the inverse of round-trip delay. We have also considered an open loop control in which the queue control threshold is dynamically adjusted according to the changes in the available bandwidth and the number of connections. This queue threshold control has been shown to be necessary and effective to prevent the ABR closed loop from converging to an undesirable equilibrium point. An extended analysis and a comprehensive cell-based simulation study for multi-hop configurations are under way and the results will be reported in a separate paper.

## References

- [1] R. Bellman, K.L. Cooke, *Differential-Difference Equations*, Academic Press, New York, 1963.
- [2] L. Benmohamed, S.M. Meerkov, Feedback control of congestion in packet switching networks: The case of single congested node, *IEEE/ACM Trans. Networking* 1(6) (1993) 693–708.
- [3] D. Bertsekas, R. Gallager, *Data Networks*, Prentice-Hall, Englewood Cliffs, NJ, 1992.
- [4] F. Bonomi, K.W. Fendick, The rate-based flow control framework for the available bit rate ATM service, *IEEE Network* 9(2) (1995) 25–39.
- [5] F. Bonomi, D. Mitra, J.B. Seery, Adaptive algorithms for feedback-based flow control in high-speed, wide-area ATM networks, *IEEE J. Select. Areas Commun.* 13(7) (1995) 1267–1283.
- [6] S. Chong, R. Nagarajan, Y.T. Wang, First-order rate-based flow control with dynamic queue threshold for high-speed wide-area ATM networks, *Proc. SPIE Conf. on Performance and Control of Network Systems*, vol. 3231, 1997, pp. 259–270.
- [7] S. Chong, Second-order rate-based flow control with dynamic queue threshold for high-speed wide-area ATM networks, preprint 1997.
- [8] A. Elwalid, Analysis of adaptive rate-based congestion control for high-speed wide-area networks, *Proc. IEEE ICC'95*, pp. 1948–1953.
- [9] E. Hernandez-Valencia et al., Rate control algorithms for the ATM ABR service, *European Trans. Telecommun.* 8(1) (1997) 7–20.
- [10] L. Kalampoukas, A. Varma, K.K. Ramakrishnan, An efficient rate allocation algorithm for ATM networks providing max–min fairness, Technical Report UCSC-CRL-95-29, Computer Engineering Dept., University of California, Santa Cruz, June 1995.
- [11] K.K. Ramakrishnan, R. Jain, A binary feedback scheme for congestion avoidance in computer networks with a connectionless network layer, *Proc. ACM SIGCOMM'88*, pp. 303–313.
- [12] S. Sathaye, ATM Forum Traffic Management Specification, Version 4.0, February 1996.
- [13] G. Stépán, *Retarded Dynamical Systems: Stability and Characteristic Functions*, Longman, New York, 1989.
- [14] N.D. Hayes, Roots of the transcendental equation associated with a certain differential-difference equation, *J. London Math. Soc.* 25 (1950) 226–232.
- [15] S. Mascola, D. Cavendish, M. Gerla, ATM rate based congestion control using a Smith predictor: An EPRCA implementation, *Proc. IEEE INFOCOM'96*, pp. 569–576.
- [16] C.E. Rohrs, R.A. Berry, A linear control approach to explicit rate feedback in ATM networks, *Proc. IEEE INFOCOM'97*, pp. 277–282.
- [17] Y. Zhao, S.Q. Li, S. Sigarto, A linear dynamic model for design of stable explicit-rate ABR control schemes, *Proc. IEEE INFOCOM'97*, pp. 283–292.
- [18] A. Kolarov, G. Ramamurthy, A control theoretic approach to the design of closed loop rate based flow control for high speed ATM networks, *Proc. IEEE INFOCOM'97*, pp. 293–301.
- [19] L. Benmohamed, Y.T. Wang, A control-theoretic ABR explicit rate algorithm for ATM switches with per-VC queueing, *Proc. IEEE INFOCOM'98*, pp. 183–191.
- [20] E. Altman, T. Basar, R. Srikant, Robust rate control for ABR services, *Proc. IEEE INFOCOM'98*, pp. 166–173.

**Song Chong** received the B.S. and M.S. degrees in Control Engineering from Seoul National University, Seoul, Korea, in 1988 and 1990, respectively, and the Ph.D. degree in Computer Engineering from the University of Texas at Austin in 1995. From 1994 to 1996, he was a Member of Technical Staff in the Performance Analysis Department at Bell Laboratories, Holmdel, New Jersey, where he worked on design and analysis of high performance broadband/ATM switches. In September 1996, he joined the Department of Electronic Engineering, Sogang University, Seoul, Korea, where he is an Assistant Professor. His current research interests are in high-speed communication networks and switching systems in general. He has published more than 20 papers in international journals and conferences and holds a U.S. patent with several pending in these areas. He is a member of IEEE and ACM and has served as a member of the Technical Program Committee for the IEEE Infocom Conference since 1997.

**Ramesh Nagarajan** is currently a member of technical staff in the Performance Analysis Department at Bell labs, Lucent Technologies. He graduated with a Ph.D. degree in Electrical and Computer Engineering from the University of Massachusetts, Amherst in 1993. His interests are in network planning and design, traffic management and data networking in general and has published several papers in these areas. He is also involved actively in the IEEE INFOCOM conference planning committees.

**Yung-Terng Wang** received the B.S. degree in Electrical Engineering from National Taiwan University in 1972 and the M.S. and Ph.D. degrees in Electrical Engineering and Computer Sciences from the University of California, Berkeley, in 1997 and 1978, respectively. He is a Technical Manager of the Performance Analysis Department at Bell Laboratories, Lucent Technologies, Holmdel, New Jersey. His current interests are in the areas of design and analysis of high performance broadband/ATM switches and networks.